Chin. J. Astron. Astrophys. Vol. 5 (2005), No. 6, 587–594
(*http://www.chjaa.org*)

Chinese Journal of
Astronomy and
Astrophysics

# Infrared Characteristics of Associated Sources of Water Masers *

Jarken Esimbek[1,2], Yue-Fang Wu[1] and Jun-Zhi Wang[1]

[1] Department of Astronomy, Peking University, Beijing 100871; *jarken@ms.xjb.ac.cn*
[2] National Astronomical Observatories/Urumqi Observatory, Chinese Academy of Sciences, Urumqi 830011

Received 2005 April 7; accepted 2005 September 16

**Abstract** We present an analysis of the infrared properties of 1417 water masers collected from the literature published by December 2004. The associated infrared sources of the water masers were identified with IRAS and MSX (Midcourse Space Experiment) catalogues. There are 1252 water masers associated with IRAS sources within $1'$, which include 700 interstellar and 552 stellar sources. For 382 sources, the IRAS counterpart identification and the maser classification are new. We found the colors of the interstellar maser sources are much redder than those of the stellar ones at IRAS wavelength bands; 99% of the interstellar maser sources are above black body line, while 95% of the stellar masers are below. The distribution difference of the two kinds of masers shown in the color-color diagram is due to their different optical depths and temperature distributions of dust regions. There are 743 water masers with MSX counterparts, of which 552 are interstellar masers and 191 are stellar masers. MSX colors of the associated sources of water masers are here analyzed for the first time. The color differences among the MSX bands are small and the interstellar masers are redder than the stellar masers. There is a correlation between the intensity of the stellar water maser emission and that of the $12\,\mu$m and $25\,\mu$m emissions, while there is no correlation between the water maser emission and the $8\,\mu$m emission. The infrared intensity increases with increasing wavelength for the interstellar masers, while it is the opposite for stellar masers. These results may provide clues for the pumping of water maser and for the properties of the two kinds of maser emission regions.

**Key words:** masers — ISM: kinematics and dynamics — stars: mass loss

## 1 INTRODUCTION

Water masers inhabit molecular clouds or circumstellar envelopes of late type stars. Their emissions have been shown to be correlated with FIR emissions, and there are two classes of masers populating different regions of the FIR color-color diagrams (Wouterloot & Walmsley 1986; Lewis & Engels 1991; Henning et al. 1990; Felli et al. 1992). The infrared characteristics

* Supported by the National Natural Science Foundation of China.

of the associated sources of masers are important for understanding maser properties and their environment. So far various criteria based on colors of IRAS sources were used to search for new water masers and to classify them (Wouterloot & Walmsley 1986; Scalise et al. 1989; Churchwell et al. 1990; Palla et al. 1991; Palagi et al. 1993). Especially, the arguments that weather water masers are pumped by radiations or collisions still exist (Rank et al. 1971; Litvak 1969; Schwartz et al. 1974; Engels et al. 1986; Elitzur 1992; Cox et al. 1978). The relation between maser emissions and infrared radiations of the associated sources may provide a channel to examine the radiation pumping mechanism.

As the number of detected water masers increases with the development of the detection technologies, the properties of the associated sources of the water maser can be examined in more detail. Particularly the newly released middle infrared data of Midcourse Space Experiment (MSX) (Egan et al. 1999) make it possible to study the properties of the associated sources of the water masers further. This paper presents the results of a check on an up-to-date sample of water masers with the IRAS-MSX data.

We describe the sample of the associated sources of water masers in Section 2. Section 3 mentions the color characters of the associated IRAS and MSX sources of the water masers. We analyze the relationship of the infrared intensities and the integrated intensities of the water masers in Section 4. A comparison of the global spectral energy distribution of the interstellar and the stellar masers is given in Section 5, and we give a brief summary in Section 6.

## 2 SAMPLE

Valdettaro et al. (2001) collected 1013 water masers with $\delta > -30^\circ$ known at April, 2000. After that there have been 32 new stellar masers collected with the Kashima 34-m radio telescope (Takaba et al. 2001), 148 water masers associated low-mass young stellar objects in Nobeyama 45-meter telescope (Furuya et al. 2003) and 16 water masers associated with low-mass protostars detected at VLA (Healy et al. 2004). Besides, 208 water maser sources were obtained in the southern hemisphere (Dinger & Dickinson 1980; Scalise et al. 1989; Batchelor et al. 1980; Caswell et al. 1983; Deguchi et al. 1989; Benson et al. 1990). So, the total number of samples we collected is 1417 up to December, 2004. Valdettaro et al. (2001) found that 937 of their 1013 sources have an IRAS counterpart within $1'$, including 410 interstellar and 460 stellar sources. We further identified associated infrared sources within $1'$. We found that, out of 1417 water masers, 1252 are, and 165 are not, associated with IRAS sources. Of the 1252 associated IRAS sources, 700 are interstellar, and 552 are stellar masers. For 382 sources, the IRAS counterpart identification and the maser classification are new. The fraction of water maser sources with IRAS counterparts is higher than that of HH objects (Wu et al. 2002).

The MSX mission surveyed the entire Galactic belt within $|b| \leq 4.5^\circ$ in five infrared bands B, A, C, D, and E, at 4, 8, 12, 15 and 21 $\mu$m (Price et al. 2001). There are 743 of the 1417 water masers associated with MSX PSC sources within $1'$. Among the 674 water masers without associated MSX point source, there are 547 with $|b| > 4.5^\circ$ and 127 objects are with $|b| < 4.5^\circ$ (see Fig. 1). The MSX survey had lower sensitivity in the B band around 4 $\mu$m (Egan et al. 1999) than in the other bands, which led to the failure of detection of most water maser sources in the B band.

## 3 COLOR CHARACTERS OF IRAS AND MSX EMISSIONS

### 3.1 Color Characters of IRAS Emissions

Figures 2a and 2b present the color-color distribution of the associated IRAS sources of water masers, with [12–60] denoting $2.5\log(F_{60}/F_{12})$ and [12–25], $2.5\log(F_{25}/F_{12})$. The symbols "•" and "△" mark the interstellar and stellar masers, respectively. The solid line is the black body

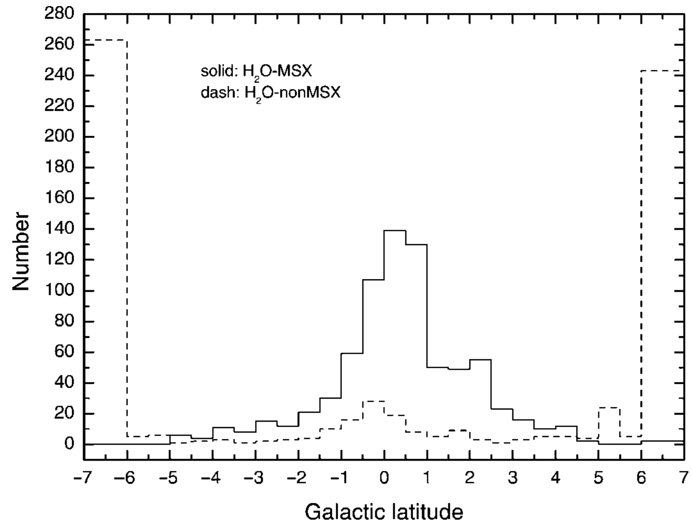


**Fig. 1** Distribution along Galactic latitude of water masers with (solid line) and without (dashed line) MSX association.

line for temperature range 90–3000 K. In Figure 2a, 691 out of the 700 interstellar masers are above the black body line, while 523 out of the 552 stellar masers are below the black body line. In Figure 2b, 695 out of the 700 interstellar masers are above the black body line, while 524 out of the 552 stellar masers are below the black body line. These results suggest that a classification with the two IRAS color indices has a 97% confidence on the whole.

The fact that the associated IRAS sources of stellar and interstellar water masers are located on different sides of the black body line in Figures 2a and 2b suggests different optical depths of dust emission and different temperature distributions around young stellar object (YSOs) and evolved stars. That the IRAS sources associated with stellar masers are below the black body line means less emission at the longer wavelengths compared to the black body profile. This can be explained with the changing of optical depth of dust emission with wavelengths. The optical depth is smaller at longer than at shorter wavelength, with $\tau(\nu) \sim \nu^{\beta}$ (normally $\beta$ is about 1–2). The flux density of the dust emission $F(\nu) \propto B(\nu, T) \times (1 - e^{-\tau(\nu)})$, $B(\nu, T)$ being the Planck function. At the long wavelength, where $\tau(\nu) < 1$, the flux density is smaller than that for the black body distribution and so the source is below the black body line in the color-color diagram. This is the case for the sources associated with stellar masers.

The sources associated with the interstellar masers lie above the black body line, which means there is more emission at the longer wavelengths compared to the black body profile. This can be explained with the temperature distribution of the dust near YSOs: a lower outside dust temperature can cause this effect. Since $\tau(\nu) \sim \nu^{\beta}$, the optical depth is less at long wavelength than at short wavelength. So the absorption of the outside dust is less at long wavelengths than at short wavelengths. In other words, the emission at the long wavelengths comes from the outside dust, while the emission at the short wavelengths comes from the inside dust. This leads to the observation that the associated sources of interstellar masers are above the black body profile in the color-color diagram (see Figs. 2a and 2b).

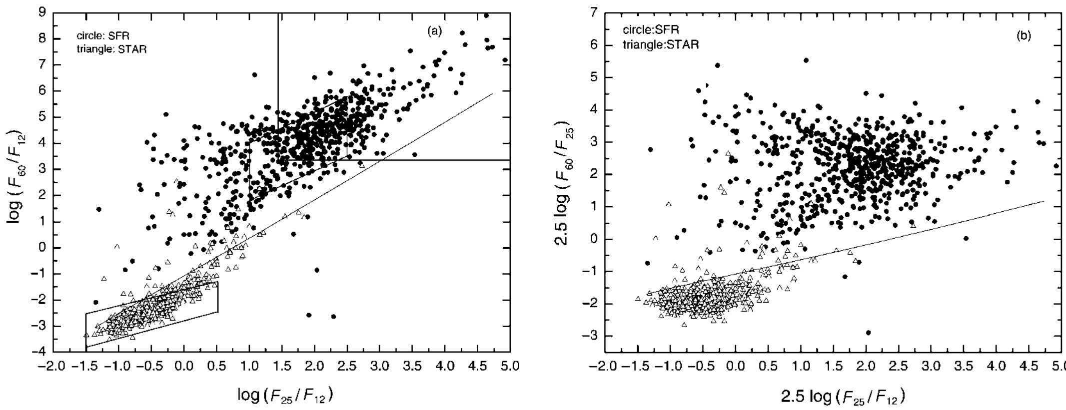


**Fig. 2** IRAS color-color diagram of the 1252 IRAS sources associated with water masers. (a) [12-25] vs. [12-60]; (b) [12-25] vs. [25-60]. In this and the following figures of present paper the symbols "•" and "△" mark the interstellar and stellar masers, respectively.

There are three different regions in the color-color diagram for water masers involving 12, 25 and 60 $\mu$m emissions (Fig. 2a). The upper-right region is the WC (Wood & Churchwell 1989) box, which is related to high mass star formation. The middle square is drawn according to the criterion of Emerson (Emerson 1987) which was intended to select low mass cloud cores. The lower-left parallelogram was drawn with the criterion of Wu et al. (1996) which is for OH/IR source candidates. We find that 70% of the interstellar masers fall in the WC region,and 58% of the same satisfied the Emerson criterion, while 87% of the stellar masers satisfy the criterion of Wu et al. These show that stellar masers are concentrated in a rather small region in the color-color diagram, suggesting that the circumstellar envelops of late type stars cover a rather small temperature range. The central region of the color-color diagram contains some sources with low color indices, and they do not belong either to interstellar or to stellar masers. However, 50% of the sources in WC and Emerson regions overlap, which suggest that both high and low-mass sources can satisfy these two color criteria. This means that it is difficult to identify the mass of the source from its color. So, it is better to estimate the mass of YSOs by their distance and radiation flux density.

### 3.2 Color Characters of MSX Emissions

The color-color diagram of MSX sources associated with water masers has been examined for the first time. As the number of the sources detected at the B band is small, we analyzed only the colors based on the A, C, D, and E bands. Figures 3a and 3b show the [C-D] vs. [C-E] and [A-D] vs. [A-E] diagrams, respectively, [C-D] $\equiv 2.5\log(F_D/F_C$, etc.). The symbols "•" and "△" mark the interstellar and stellar masers, respectively. The solid line is the black body line for temperatures from 140 K to infinity.

There are 240 interstellar and 138 stellar maser sources detected at MSX C, D and E bands and 286 interstellar masers and 141 stellar maser sources at MSX A, D and E bands. The difference in MSX color range between the interstellar and stellar masers as shown in Figures 3a and 3b is smaller than that in IRAS color range as shown in Figures 2a and 2b. Still, one can see that, here, in Figures 3a and 3b, the color range of the stellar maser sources is smaller than that of the interstellar masers, suggesting again that the temperature range of the

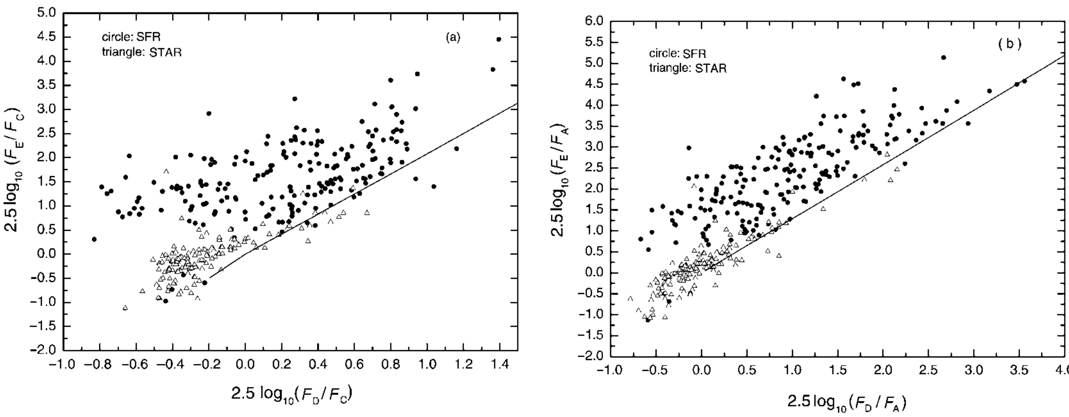


**Fig. 3** MSX color-color diagram (a) [C-D] vs. [C-E] of 378 MSX sources associated with water masers; (b) [A-D] vs. [A-E] of the 461 MSX sources associated with water masers.

former is smaller than the latter. Also, the difference between the distribution of the two kinds of masers relative to the black body line is less than in the IRAS color-color diagrams. This is due to the emission tends to be the same in the middle infrared wavelength (see Sect. 5).

## 4 THE RELATIONSHIP BETWEEN THE INTENSITY OF WATER MASER EMISSION AND THE IRRADIATION BY THE ASSOCIATED INFRARED SOURCE

To investigate the possibility of infrared pumping of water masers, we analyse the relationship between the integrated flux of the interstellar water maser and the flux of the associated IRAS source at different wavelength. Figures 4a and 4b plot the integrated maser flux against the 12 $\mu$m and 25 $\mu$m flux densities of the associated IRAS source. Linear fittings for the two plots are $\log F = 1.55(\pm 0.07) + 0.20(\pm 0.07) \log F_{12}$ and $\log F = 1.25(\pm 0.12) + 0.29(\pm 0.07) \log F_{25}$, respectively. The linear correlation coefficients are 0.21 and 0.29, indicating that there are no correlation between interstellar water masers and infrared 12 and 25 $\mu$m photons.

Figures 5a and 5b plot the integrated flux of the stellar water maser sources and the IRAS flux density at 12 $\mu$m and 25 $\mu$m. The fitting results are $\log F = 0.57(\pm 0.17)+0.47(\pm 0.09) \log F_{12}$ and $\log F = 0.60(\pm 0.15) + 0.51(\pm 0.09) \log F_{25}$ . The linear correlation coefficients are 0.52 and 0.58, respectively, which is better than in the interstellar case. These results indicate that some correlation exists between stellar water masers and infrared 12 $\mu$m and 25 $\mu$m photons. We suggest that the infrared radiation at 12 and 25 $\mu$m plays some role in stellar water maser process. However, these results are not enough to prove that the stellar water masers are excited by infrared radiation.

Figure 6a shows the relationship between interstellar maser flux and MSX A band flux. The correlation coefficient of a linear fit is –0.07. Figure 6b shows the relationship between stellar maser flux and MSX A band flux. The correlation coefficient of a linear fit is 0.15. These results show that there is no correlation between the integrated flux of either interstellar or stellar water masers and the MSX A band flux. This suggests that the interstellar and stellar water masers may not be excited by 8 $\mu$m photons. On the other hand, SiO masers do show a correlation with the 8 $\mu$m MSX emission (Jiang 2002).

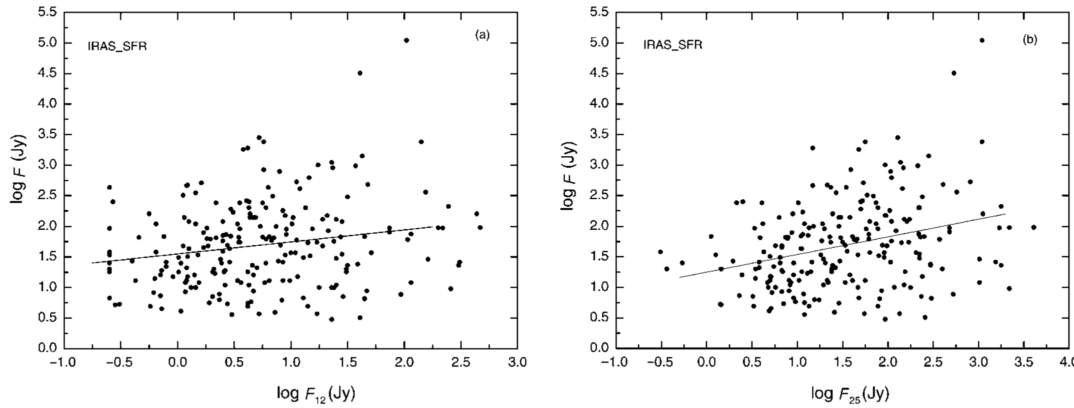


**Fig. 4** (a) Integrated flux of interstellar maser sources vs. flux density of IRAS sources at $12\,\mu$m of the associated maser sources; (b) Same as (a) but at $25\,\mu$m.

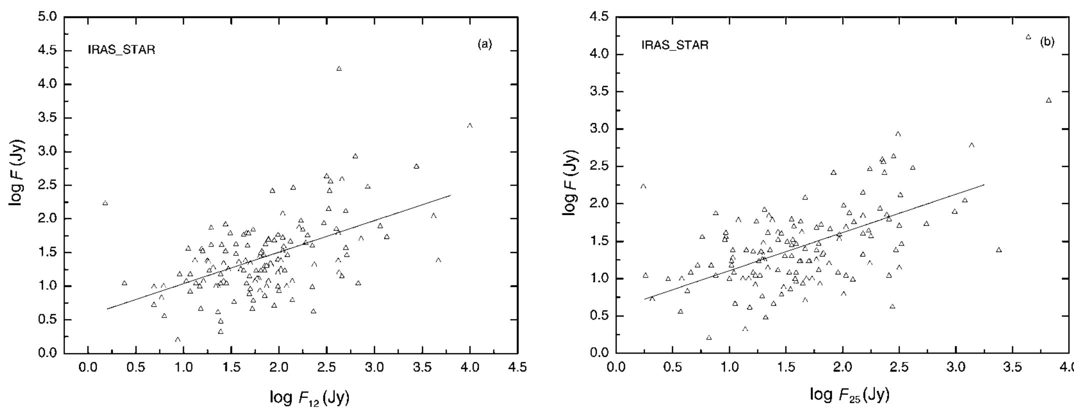


**Fig. 5** (a) Integrated flux of stellar maser sources vs. flux density of IRAS sources at $12\,\mu$m of the associated maser sources; (b) Same as (a) but at $25\,\mu$m.

## 5 DIFFERENCE BETWEEN THE AVERAGE SPECTRA OF INTERSTELLAR AND STELLAR WATER MASERS

Among 743 water maser sources (of which 552 are interstellar and the remaining are stellar ones) 90 were detected in $B_1$ and 710 were detected at A band, with the $B_1$ flux lower due to its narrower bandwidth. Of the 552 interstellar water masers 232 are detected in all four MSX bands. The average intensities of the interstellar masers at the MSX and IRAS bands are plotted in Figure 7 with the solid line. Here 156 of 191 stellar sources were detected in the four MSX bands and the four IRAS bands emission. The dashed line in Figure 7 shows the average intensity of these stellar masers. From Figure 7, one can see that the mid-far infrared flux of the interstellar sources increases with increasing wavelengths, while that of the stellar masers is flat and very weak. Figure 7 also shows between 15–25$\,\mu$m the intensities of the two kind sources tend to be equal.

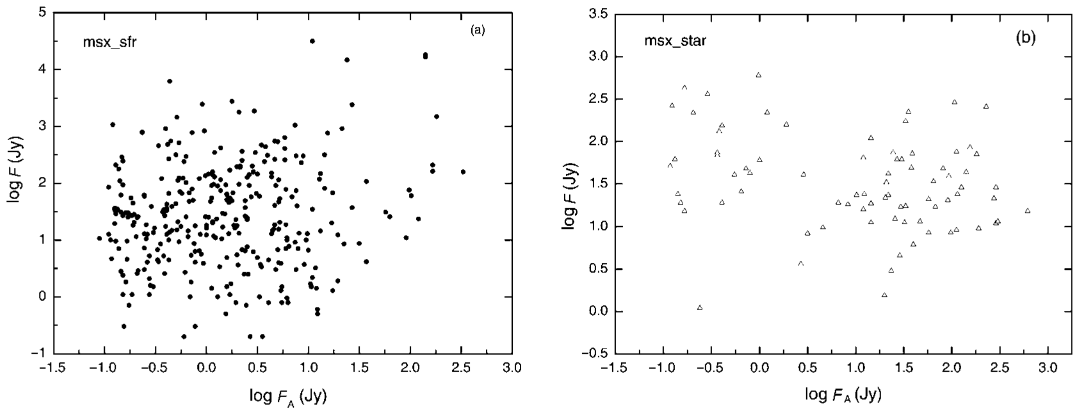


**Fig. 6** (a) Integrated flux of interstellar maser emission vs. MSX flux density at MSX A band; (b) Same as (a) but for stellar masers.

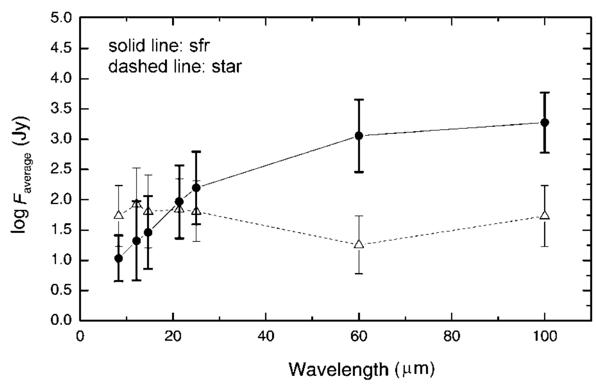


**Fig. 7** A plot of average intensity of interstellar and stellar water maser sources at the MSX A, C, D, E and the four IRAS bands.

## 6 SUMMARY

We have collected 1417 water masers from both the northern and southern hemispheres and reclassified them into two classes: interstellar and stellar water masers. Their associated sources are identified with the IRAS and MSX point source catalog, and their colors in both the IRAS and MSX wavelength bands are examined. The main results are as follows:

(1) The number of water masers associated with IRAS sources within $1'$ is 1252, including 700 interstellar and 552 stellar masers.
(2) In the color-color diagram, the region of distribution is more extended for the interstellar masers than for the stellar masers, showing that the temperature range of interstellar masers is larger than that of stellar masers. We found 99% of the interstellar sources are above the black body line, while 95% of the stellar sources are below the line. The difference in distribution in the color-color diagram is due to their different optical depths and temperature distributions of the dust region.

(3) In the color-color diagrams of MSX A, C, D, E bands the distribution difference of the two kinds of maser sources is less than that in the IRAS color-color diagrams.
(4) The correlation between the water emission intensity and the flux density at 12 $\mu$m and 25 $\mu$m is better for the stellar maser sources than for the interstellar ones, showing that the infrared radiation at 12 $\mu$m and 25 $\mu$m plays some role in stellar water maser process. However, these results are not enough to prove that the stellar water masers are excited by infrared radiation.
(5) The infrared intensity of interstellar maser sources increases with increasing wavelength, while for the stellar ones there is no obvious variation. In the 15–25 $\mu$m wavelength range the intensities of the two kinds of sources tend to be equal.

**Acknowledgements** This project is supported by the NSFC Grant Nos., 10203003, 10133020, 10128306, NKBRSF G1999075405, and the United Astronomy Laboratory of CAS.

## References

Batchelor R. A., Caswell J. L., Haynes R. F. et al., 1980, Aust. J. Phys., 33, 139
Benson P. J., Little-Marenin I. R., Woods T. C. et al., 1990, ApJS, 74, 911
Caswell J. L., Batchelor R. A., Forster J. R. et al., 1983, Aust. J. Phys., 36, 401
Churchwell E., Walmsley C. M., Cesaroni R., 1990, A&AS, 83, 119
Cox G. G., Parker E. A., 1978, MNRAS, 183, 111
Deguchi S. H., Nakada Y., Forster J. R., 1989, MNRAS, 239, 825
Dinger A. C., Dickinson D. F., 1980, AJ, 85, 1247
Egan M. P., Price S. D., Moshir M. M. et al., 1999, Technical Report, AD-A381933; AFRL-VS-TR-1999-1522
Engels D., Schmid -Burgk J., Walmsley C. M., 1986, A&A, 167, 129
Elitzur M., Astronomical Masers, 1992, Kluwer Academic Publishers
Emerson J. P., 1987, IAUS, 115, 19
Felli M., Palagi F., Tofani G., 1992, A&A, 255, 293
Furuya R. S., Kitamura Y., Wootten A. et al., 2003, ApJS, 144, 71
Henning T., Pfau W., Altenhoff W. J., 1990, A&A, 227, 542
Jiang B. W., 2002, ApJ, 566, 37
Healy K. R., Hester J. J., Claussen M. J., 2004, ApJ, 610, 835
Kruegel E., Walmsley C. M., 1984, A&A, 130, 5
Lewis B. M., Engels D., 1991, MNRAS, 251, 39
Litvak M. M., 1969, Science, 165, 855
Mezger M. P., Mathis J. S., Panagia N., 1982, A&A, 105, 372
Palagi F., Cesaroni R., Comoretto G. et al., 1993, A&AS, 101, 153
Palla F., Brand J., Comoretto G. et al., 1991, A&A, 246, 249
Price S., Egan E., Carey S. et al., 2001, AJ, 121, 2819
Mezger M. P., Mathis J. S., Panagia N., 1982, A&A, 105, 372
Rank D. H., Townes C. H., Welch W. J., 1971, Science, 174, 1083
Scalise E. Jr., Rodriguez L. F., Mendoza-Torres E., 1989, A&A, 221, 105
Schwartz P. R., Harvey P. M., Barrett A. H., 1974, ApJ, 187, 491
Takaba H., Iwata T., Miyaji T., Degichi S. H., 2001, PASJ, 53, 517
Valdettaro R., Palla F., Brand J. et al., 2001, A&A, 368, 845
Wood D. O. S., Churchwell E., 1989, ApJ, 340, 265
Wouterloot J. G. A., Walmsley C. M., 1986, A&A, 168, 237
Wu Y., Mao R., Lu J. et al., 1996, In: N. Kaifu ed., Ground-Based Astronomy in Asia, Proceedings of the Third East-Asian Meeting on Astronomy, Japan: Tokyo, p.167
Wu J., Wu Y., Wang J. et al., 2002, ChJAA, 2, 33